Evgeny V. Nazarchuk, Oleg I. Siidra*, Dmitri O. Charkin and Yana G. Tagirova

# A new uranyl silicate sheet derived from phosphuranylite topology in the structure of $Cs_4[(UO_2)_5(SiO_3OH)_2O_2F_4]$

https://doi.org/10.1515/zkri-2023-0038
Received September 9, 2023; accepted March 20, 2024;
published online April 17, 2024

**Abstract:** A new uranyl silicate $Cs_4[(UO_2)_5(SiO_3OH)_2O_2F_4]$ (**1**), was obtained via a hydrothermal route. The new compound is monoclinic, $P2_1/n$, $a$ = 8.3870(2), $b$ = 13.4612(2), $c$ = 10.9503(2) Å, $\beta$ = 91.223(2)°, $V$ = 1236.00(4) Å$^3$; the structure has been solved and refined down to $R_1$ = 0.022. Therein, the phosphouranylite units (***PU***s) associate into a new type of uranyl-silicate layers, $[(UO_2)_5(SiO_3OH)_2O_2F_4]^{4-}$, which interleave with the $Cs^+$ cations. Topological analysis of ***PU*** based structures indicates that these layers in **1** provide a unique example of complexes constructed only via association of the ***PU*** and not involving other building units.

**Keywords:** uranyl oxysalts; silicates; inorganic synthesis; phosphouranylite

## 1 Introduction

Uranium silicates attract attention as important constituents, on the one hand, of oxidation areas of uranium deposits [1, 2] and, on the other hands, of deposited radioactive wastes, as well as novel functional materials [3]. The diversity of their crystal structures is generally underpinned by the ability of the silicate tetrahedra to polymerize into numerous anions of varied size, topology, and dimensionality [3, 4]. In the majority of known cases, linkage of $UO_n$ and $SiO_4$ polyhedra results in the formation of framework structures [5], including nanotubular [6]. A variety of synthetic protocols have been successfully employed in preparation of these compounds, including soft [7] and harsh [8] hydrothermal procedures, as well as crystallization from melts [9] and fluxes [10]. Recently, we have demonstrated that silica tubes can be effectively used as the silicate source [11].

Despite the known anisotropy of bond distances for uranyl compounds [4] and the diversity of synthetic approaches, layered uranyl silicates remain rather uncommon. The most frequently observed 2*D* complex among natural uranyl silicates is the uranophane-like layer [12], first reported for the structure of α-uranophane, $Ca[(UO_2)_2(SiO_3OH)_2](H_2O)_5$ [13]. As of today, this group contains nine minerals contributing to several topological isomers [12] which differ by the orientation of terminal vertices of the silicate tetrahedra. Note that in eight structures (out of nine) this vertex is protonated, except for kasolite $Pb[(UO_2)(SiO_4)](H_2O)$ [14].

A layered structure has also been observed for another uranyl silicate mineral, haiweeite $Ca[(UO_2)_2(Si_5O_{12})(OH)_2](H_2O)_6$ [15] wherein the uranyl polyhedra arrange in chains similar to those in uranophane, while the $SiO_4$ tetrahedra condense into complex chains which finally results in formation of $[(UO_2)_2Si_5O_{12}(OH)_2]^{2-}$ layers.

Complex "double-decker" $[(UO_2)_3(Si_2O_7)_2]^{6-}$ layers were found in the structures of $Na_6[(UO_2)_3(Si_2O_7)_2]$ [16], $Na_3K_3[(UO_2)_3(Si_2O_7)_2](H_2O)_2$, and $Na_3Rb_3[(UO_2)_3(Si_2O_7)_2]$ [17]. In contrast to the previous cases, therein the uranium centers a tetragonal pyramid (a squeezed octahedron), and the $SiO_4$ tetrahedra form the *diortho* $Si_2O_7^{6-}$ groups. Further polymerization leads to $[(UO_2)(Si_2O_6)]^{2-}$ layers, as in the structure of $Ba[(UO_2)(Si_2O_6)]$ [18].

In the current paper, we report a new result of our search for new uranyl silicates, the synthesis, crystal structure, and topological analysis of a novel compound $Cs_4[(UO_2)_5(SiO_3OH)_2O_2F_4]$ (**1**).

## 2 Experimental

Caution! Although the uranium precursors used contain depleted uranium, standard safety measures for handling radioactive substances must be followed.

### 2.1 Synthesis

Yellow plate-like crystals of **1** were obtained starting from a mixture of 1.49 g $U_3O_8$ (Vecton, 99.7 %), 0.12 g $SiO_2$ (Vecton, 99.7 %), and 0.67 g CsCl

***Corresponding author: Oleg I. Siidra**, Department of Crystallography, Saint-Petersburg State University, University emb. 7/9, St. Petersburg 199034, Russia; and Kola Science Center, Russian Academy of Sciences, Apatity, Murmansk Region, 184200, Russia, E-mail: o.siidra@spbu.ru
**Evgeny V. Nazarchuk and Yana G. Tagirova**, Department of Crystallography, Saint-Petersburg State University, University emb. 7/9, St. Petersburg 199034, Russia
**Dmitri O. Charkin**, Department of Chemistry, Moscow State University, Vorobievy Gory 1, bd. 3, Moscow 119991, Russia

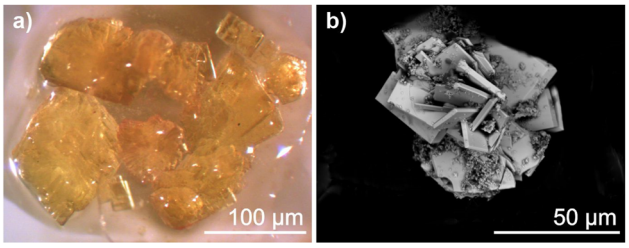


**Figure 1:** Yellow crystals and SEM image of $Cs_4[(UO_2)_5(SiO_3OH)_2O_2F_4]$.

(Vecton, 99.7 %), which was transferred into 5 ml distilled water to which 1 ml 40 % HF was added. The molar ratio of $U_3O_8$:$SiO_2$:CsCl was 1:1:2. The slurry was transferred into a PFTE lined 20 ml steel autoclave and heated to 220 °C, soaked for 72 h, and cooled to room temperature at a rate of 5 °C/h. The transparent yellow solution was poured into a plastic Petri dish in a fume hood within 10 h. Druses of crystals were formed (Figure 1). The estimated yield is *ca.* 30 %; the mother liquor turned viscous upon further evaporation, produced no more crystals and was finally discarded.

### 2.2 Single-crystal X-ray studies

Single-crystal X-ray data of **1** were collected using a Rigaku XtaLAB Synergy-S diffractometer equipped with a PhotonJet-S detector operating with MoKα radiation at 50 kV and 1 mA. A single crystal was chosen and more than a hemisphere of data collected with a frame width of 0.5° in *ω*, and 20 s spent counting for each frame. The data were integrated and corrected for absorption applying a multi-scan type model using the Rigaku Oxford Diffraction programs CrysAlis Pro [19]. The unit cell parameters were calculated by the least-squares method. The structures were solved by direct methods using WinGX [20] and Olex2 [21] software. The parameters of the X-ray diffraction experiment and structure refinement are given in Table 1. The final model of **1** includes the coordinates and anisotropic thermal parameters of atoms. Selected interatomic distances are collected in Table S1. The calculated bond-valence sums (Table 2) are in general agreement with the expected oxidation states for all atoms. The bond valence sums were calculated using the parameters from [22–24].

Qualitative electron microprobe analysis of (**1**) (Hitachi TM 3000) revealed no other elements, except U, Si, Cs, O and F.

**Table 1:** Crystallographic data and refinement parameters for $Cs_4[(UO_2)_5(SiO_3OH)_2O_2F_4]$.

| | |
|---|---|
| Crystal system | monoclinic |
| Space group | $P2_1/n$ |
| *a* (Å) | 8.3870(2) |
| *b* (Å) | 13.4612(2) |
| *c* (Å) | 10.9503(2) |
| *β* (°) | 91.223(2) |
| Volume (Å$^3$) | 1236.00(4) |
| $D_{calc}$ (g/cm$^3$) | 5.841 |
| $\mu$ (mm$^{-1}$) | 38.656 |
| Crystal size (mm) | 0.03 × 0.31 × 0.25 |
| Radiation | MoKα |
| Temperature (K) | 100 |
| *h*, *k*, *l* ranges | −13 → 12 |
| | −20 → 19 |
| | −16 → 15 |
| Total reflections collected | 4379 |
| Unique reflections ($R_{int}$) | 3862 (0.0291) |
| $R_1[F > 4\sigma F]$, w$R_1[F > 4\sigma F]$ | 0.0223, 0.0388 |
| $R_{all}$, w$R_{all}$ | 0.0307, 0.0403 |
| Goodness-of-fit | 1.042 |
| CCDC number | 2290318 |

## 3 Results and discussion

### 3.1 Structure description

In the crystal structure of (**1**), three uranium atoms form a typical uranyl (*Ur*) cation (<U-$O_{ap}$> = 1.801, 1.808 and 1.811 Å for U1, U2 and U3 respectively). The *Ur*1 in the equatorial plane is coordinated by six oxygen atoms (<U-$O_{eq}$> = 2.489 Å) to form *Ur*1$O_6$ polyhedra. The *Ur*2 and *Ur*3 are coordinated by three oxygen (<U2-$O_{eq}$> = 2.323, <U3-$O_{eq}$> = 2.312 Å) and two fluorine (<U2-$F_{eq}$> = 2.327 Å, <U3-$F_{eq}$> = 2.333 Å) atoms thus forming *Ur*2$O_3F_2$ and *Ur*3$O_3F_2$ polyhedra, respectively (Figure 2).

One symmetrically independent silicon atom is tetrahedrally coordinated by three oxygen atoms (<Si–O> = 1.621 Å) and one $OH^-$ group (Si–OH = 1.643(4) Å) to form $SiO_3OH$ polyhedra (Figure 2). Two cesium atoms are coordinated, at distances below 3.5 Å, by 9 and 10 ligands to form Cs1$O_8$OH and Cs2$O_7F_2$OH polyhedra.

In the structure of (**1**), the *Ur*1$O_6$ polyhedra share edges with two *Ur*2$O_3F_2$ and two *Ur*3$O_3F_2$ polyhedra to form $[(UO_2)_5O_8F_8]^{16-}$ units. Two $SiO_3OH$ tetrahedra share edges with *Ur*1$O_6$ polyhedra to form $[(UO_2)_5(SiO_3OH)_2O_4F_8]^{12-}$ phosphuranylite units (***PU***) [25, 26] (Figure 2). These share fluorine vertices of the *Ur*2$O_3F_2$ and *Ur*3$O_3F_2$ polyhedra to form the $[(UO_2)_5(SiO_3OH)_2O_2F_4]^{4-}$ layers (Figure 3a) which interleave with cesium cations (Figure 3b).

### 3.2 Discussion

The complexes formed via association of the ***PU*** units are commonly observed among uranium compounds (Table S2). Most common are those with the phosphuranylite sheet-anion topology $[(UO_2)_3(TO_4)_2X_2]$, where *T* = P, As, Se and *X* = O or OH (Figure 4a). Their diversity comes from both the substitution at the *T* site and the orientational variation of the terminal vertices of the tetrahedra [4]. Besides $P^V$, $As^V$, and $Se^{VI}$ centering the $TO_4$ tetrahedra, the *T* site can be

**Table 2:** Bond-valence values[a] for $Cs_4[(UO_2)_5(SiO_3OH)_2O_2F_4]$.

| | O1 | O2 | O3 | O4 | O5 | O6 | O7 | O8 | OH1 | O10 | F1 | F2 | ∑vc |
|---|---|---|---|---|---|---|---|---|---|---|---|---|---|
| U1 | 1.68 × 2 | | | | | | 0.26 × 2 | 0.39 × 2 | | 0.59 × 2 | | | 5.84 |
| U2 | | 1.65 | 1.66 | | | 0.39 | 0.6 | | | 0.73 | 0.42 | 0.42 | 5.87 |
| U3 | | | | 1.67 | 1.63 | 0.45 | | 0.57 | | 0.72 | 0.44 | 0.39 | 5.87 |
| Si1 | | | | | | 1.02 | 1.01 | 0.99 | 0.95 | | | | 3.97 |
| Cs1 | 0.11 | 0.15 | 0.1 | 0.19 | 0.07 | 0.09 | | 0.1 | 0.11 | | | | 1.01 |
| | | 0.09 | | | | | | | | | | | |
| Cs2 | 0.15 | 0.06 | 0.11 | 0.09 | 0.09 | | 0.09 | | 0.06 | | 0.14 | 0.08 | 0.99 |
| | | | 0.08 | | | | | | | | | 0.04 | |
| ∑va | 1.94 | 1.95 | 1.95 | 1.95 | 1.79 | 1.95 | 1.96 | 2.05 | 1.12 | 2.04 | 1.00 | 0.93 | |

[a]Expressed in valence units (*vu*).

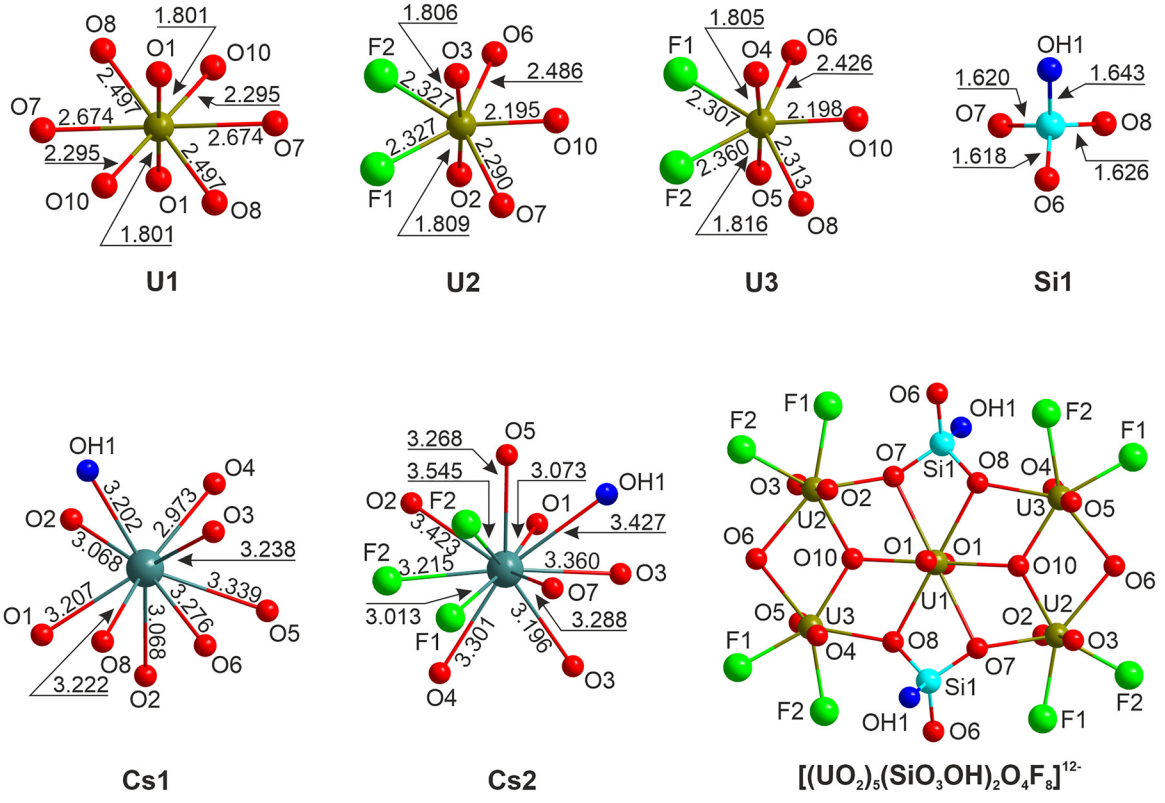


**Figure 2:** The crystal structure of $Cs_4[(UO_2)_5(SiO_3OH)_2O_2F_4]$ . $[(UO_2)_5(SiO_3OH)_2O_2F_4]^{4-}$ layers in *ac* plane (a). General projection of the crystal structure of $Cs_4[(UO_2)_5(SiO_3OH)_2O_2F_4]$ along the *b* axis (b) ($UO_n$ polyhedra = orange, $SiO_3OH$ = blue, Cs = cyan balls, F = green balls).

occupied by $Se^{IV}$ and $C^{IV}$ forming ψ-tetrahedral and trigonal planar anions, respectively.

Besides phosphuranylite, there are some other topologies known also based on the ***PU*** units. In the structure of $Cs_2(H_2O)_5[(UO_2)_7(SeO_4)_2(SeO_3)_2O_4]$ [25], the Se atoms adopt two coordinations: $Se^{IV}O_3$ and $Se^{VI}O_4$ (Figure 4b). Therein, the ***PU*** units are arranged into layers by the means of $\{(UO_2)_2(Se^{VI}O_4)_4O_4\}$ linkers. In the structures of $Rb_6[(UO_2)_7(PO_4)_4O_4]$ and $Rb_6[(UO_2)_7(AsO_4)_4O_4]$ [26], the $[(UO_2)_7(PO_4)_4O_4)]^{6-}$ layers are formed according to a relatively rare association mechanism via cation-cation interaction of uranyl polyhedra [6] (Figure 4c). Linkage of ***PU*** units by $\{(UO_2)_2(TO_4)_2O_4\}$ groups leads to chains stitched into layers via the cation-cation interaction. An example of ***PU*** assembling into chains is the structure of kamitugaite, $PbAl[(UO_2)_5(PO_4)_{2.38}(AsO_4)_{0.62}O_2(OH)_2](H_2O)_{11.5}$ [27] (Figure 4d), but even then they are linked via "extra" phosphate groups. A similar pattern is observed in the structure of $(C_{10}H_9N_2)_3[(UO_2)_5(HPO_4)_3(PO_4)F_4]$ [28]. In the $[(UO_2)_5(HPO_4)_3(PO_4)F_4]^{3-}$ layers (Figure 4e), the ***PU*** units assemble via two "extra" $PO_4$ tetrahedra. Note that in this case the uranyl cations adopt a mixed-ligand O/F

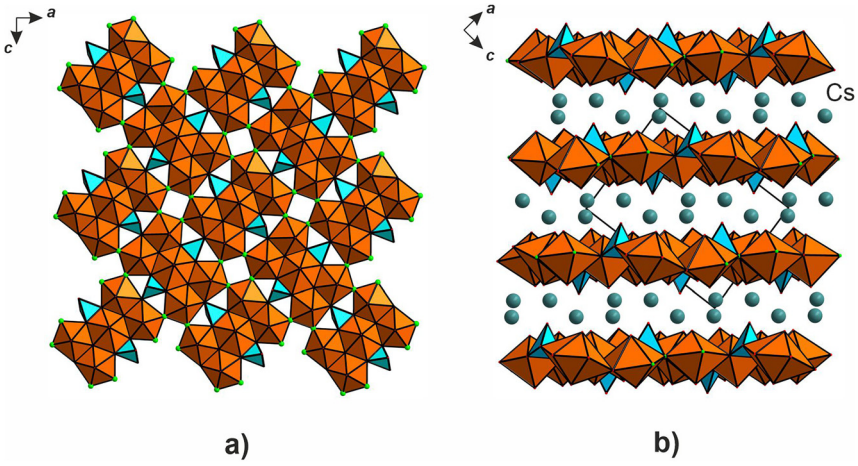


**Figure 3:** Layers in the structure of $Cs_4[(UO_2)_5(SiO_3OH)_2O_2F_4]$ (a). General projection of the structure along the *b* axis (b) ($UO_n$ polyhedra = orange, $SiO_3OH$ = blue, Cs = cyan balls, F = green balls).

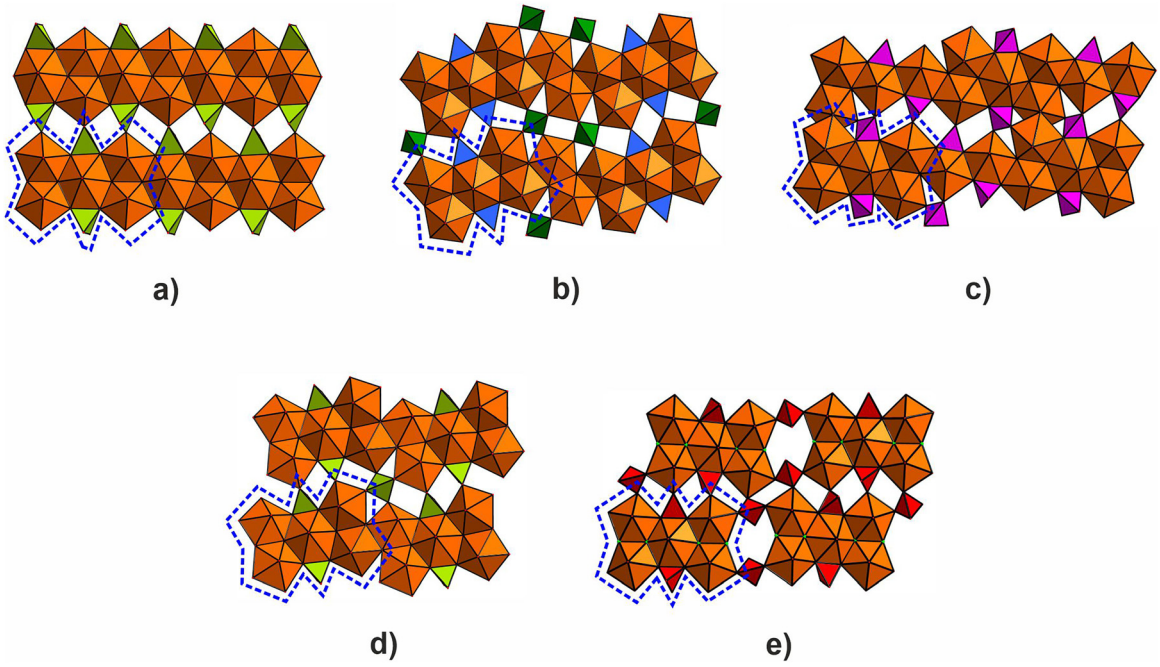


**Figure 4:** Structural units derived from phosphuranylite topology in uranyl oxysalts (***PU*** units are highlighted by blue dotted lines). $[(UO_2)_3(TO_4)_2X_2]$ ($T$ = P, As; $X$ = O or OH) layer ($TO_4$ = green) in phosphuranylite group minerals (a), $[(UO_2)_7(SeO_4)_2(SeO_3)_2O_4]$ layer ($SeO_4$ =green; $SeO_3$ = blue) in $Cs_2(H_2O)_5[(UO_2)_7(SeO_4)_2(SeO_3)_2O_4]$ (b), $[(UO_2)_7(PO_4)_4O_4]$ layer ($PO_4$ =purple) in $Rb_6[(UO_2)_7(PO_4)_4O_4]$ (c), $[(UO_2)_5(PO_4)_{2.38}(AsO_4)_{0.62}O_2(OH)_2]$ layer ($TO_4$ = green) in $PbAl[(UO_2)_5(PO_4)_{2.38}(AsO_4)_{0.62}O_2(OH)_2](H_2O)_{11.5}$ (d) and $[(UO_2)_5(HPO_4)_3(PO_4)F_4]$layer ($TO_4$ = red) in $(C_{10}H_9N_2)_3[(UO_2)_5(HPO_4)_3(PO_4)F_4]$ (e) layers. See the text for details.

coordination and share common F···F edges. The structures of nielsbohrite, $K[(UO_2)_3(AsO_4)(OH)_4](H_2O)$ [29], and a synthetic compound $[(UO_2)_3(PO_4)O(OH)(H_2O)_2](H_2O)$ [30] are microporous. In these frameworks, the chains formed by ***PU*** units and $\{(UO_2)_2(TO_4)_4O_4\}$ units are formed.

Therefore, in all hitherto reported structures the ***PU*** units are linked into layers or frameworks by some "extra" species. In contrast, the structure of **1** is the first wherein the layers are formed without any additional linkers. The difference in topology comes not only from the geometry of the $TO_4$ (or $TO_3$) polyhedra, but also from the nature of the $T$ cations. The $TO_4$ ($TO_3$) and $UO_n$ polyhedra share vertices and edges; therefore, the separations between the chains formed by ***PU*** are dictated by the size of $TO_m$ polyhedra. Of more importance is the size agreement between the edges of $UO_n$ (2.410–2.502 Å in the equatorial plane) and the $TO_m$ poyhedra ($PO_4^{3-}$: 2.308–2.564 Å, $AsO_4^{3-}$: 2.428–2.546 Å, $SiO_4^{4-}$: 2.466–2.730 Å, $SeO_3^{2-}$: 2.502–2.676 Å). This determines whether the $UO_n$ and $TO_m$ polyhedra would share only vertices ($\kappa^1$ coordination) or also edges ($\kappa^2$ coordination). The latter mode corresponds to essentially closer U···$T$ separations and consequently stronger Coulombic repulsion. The

smaller the size of *T* and the higher its charge, the less favorable is the $\kappa^2$ coordination. The relatively small charge of $Si^{IV}$ makes such coordination possible which provides a further contribution to the diversity of structural chemistry of uranyl silicates.

By now, fluorine-bearing ***PU*** units have been reported for three compounds: $A_{4.4}K_{0.6}[(UO_2)_6O_4F(PO_4)_4(UO_2)]$ (A = Rb, Cs [31]), and $(C_{10}H_9N_2)_3[(UO_2)_5(HPO_4)_3(PO_4)F_4]$ [28]. In the first two cases, exact positions of the $F^-$ anions could not be localized and mixed O/F occupancies have been suggested. This can be explained considering the high-temperature conditions. In our case, as well as in that of $(C_{10}H_9N_2)_3[(UO_2)_5(HPO_4)_3(PO_4)F_4]$, synthesis conditions provided complete ordering of the O and F sites. The mechanism of F-bearing architecture formation and association in solutions remains obscure; yet one can suggest that these clusters may initially be formed in the mother liquors or melts, "stitched" by various linkers present therein. In our case, the $F^-$ anions may have played the linker role.

**Acknowledgements:** We are grateful to two anonymous reviewers for valuable comments. Technical support by the X-Ray Diffraction and Geomodel Resource Centers of Saint-Petersburg State University is gratefully acknowledged.
**Research ethics:** Not applicable.
**Author contributions:** The authors have accepted responsibility for the entire content of this manuscript and approved its submission.
**Competing interests:** The authors state no conflict of interest.
**Research funding:** The Russian Science Foundation through the grant 23-27-00153 (E.V.N. and Y.G.T.).
**Data availability:** The raw data can be obtained on request from the corresponding author.

# References

1. Belova L. N., Doynikova O. A. Formation conditions of uranium minerals in oxidation zone of uranium deposits. *Geol. Ore Deposit.* 2003, *45*, 130–132.
2. Plášil J. Mineralogy, crystallography and structural complexity of natural uranyl silicates. *Minerals* 2018, *8*, 551.
3. Burns P. C., Olson R. A., Finch R. J., Hanchar J. M., Thibault Y. $KNa_3(UO_2)_2(Si_4O_{10})_2(H_2O)_4$, a new compound formed during vapor hydration of an actinide-bearing borosilicate waste glass. *J. Nucl. Mater.* 2000, *278*, 290–300.
4. Lussier A. J., Lopez R. A. K., Burns P. C. A revised and expanded structure hierarchy of natural and synthetic hexavalent uranium compounds. *Can. Mineral.* 2016, *54*, 177–283.
5. Nazarchuk E. V., Siidra O. I., Charkin D. O., Tagirova Y. G. Framework uranyl silicates: crystal chemistry and a new route for the synthesis. *Materials* 2023, *16*, 4153.
6. Nazarchuk E. V., Siidra O. I., Charkin D. O., Tagirova Y. G. Uranyl silicate nanotubules in $Rb_2[(UO_2)_2O(Si_3O_8)]$: synthesis and crystal structure. *Z. Kristallogr.* 2023, *238*, 349–354.
7. Huang J., Wang X., Jacobson A. J. Hydrothermal synthesis and structures of the new open-framework uranyl silicates $Rb_4(UO_2)_2(Si_8O_{20})$ (USH-2Rb), $Rb_2(UO_2)(Si_2O_6)H_2O$ (USH-4Rb) and $A_2(UO_2)(Si_2O_6)\cdot 0.5H_2O$ (USH-5A.; A = Rb, Cs). *J. Mater. Chem.* 2003, *13*, 191–196.
8. Liu H. K., Peng C. C., Chang W. J., Lii K. H. Tubular chains, single layers, and multiple chains in uranyl silicates: $A_2[(UO_2)Si_4O_{10}]$ (*A* = Na, K, Rb, Cs). *Cryst. Growth Des.* 2016, *9*, 5268–5272.
9. Morrison G., Smith M. D., Tran T. T., Halasyamani P. S., zur Loye H. C. Synthesis and structure of the new pentanary uranium(vi) silicate, $K_4CaUSi_4O_{14}$, a member of a structural family related to fresnoite. *CrystEngComm* 2015, *17*, 4218–4224.
10. Lee C., Wang S., Chen Y., Lii K. Flux synthesis of salt-inclusion uranyl silicates: $[K_3Cs_4F]$ $[(UO_2)_3(Si_2O_7)_2]$ and $[NaRb_6F]$ $[(UO_2)_3(Si_2O_7)_2]$. *Inorg. Chem.* 2009, *48*, 8357–8361.
11. Nazarchuk E. V., Siidra O. I., Charkin D. O., Tagirova Y. G. U(VI) coordination modes in complex uranium silicates: $Cs[(UO_6)_2(UO_2)_9(Si_2O_7)F]$ and $Rb_2[(PtO_4)(UO_2)_5(Si_2O_7)]$. *Chemistry* 2022, *4*, 1515–1523.
12. Burns P. C. $U^{6+}$ minerals and inorganic compounds: insights into an expanded structural hierarchy of crystal structures. *Can. Mineral.* 2005, *43*, 1839–1894.
13. Websky M. Ueber die geognostischen verhältnisse der erzlagerstätten von kupferberg und rudelstadt in schlesien. *Z. Geol. Gesell.* 1985, *5*, 373–438.
14. Fejfarová K., Dušek M., Plášil J., Čejka J., Sejkora J., Škoda R. Reinvestigation of the crystal structure of kasolite, $Pb[(UO_2)(SiO_4)](H_2O)$, an important alteration product of uraninite, $UO_{2+x}$. *J. Nucl. Mater.* 2013, *434*, 461–467.
15. Plášil J., Fejfarova K., Cejka J., Dusek M., Skoda R., Sejkora J. Revision of the crystal structure and chemical formula of haiweeite, $Ca(UO_2)_2(Si_5O_{12})(OH)_2\times 6H_2O$. *Am. Mineral.* 2013, *98*, 718–723.
16. Li H., Langer E. M., Kegler P., Alekseev E. V. Structural and spectroscopic investigation of novel 2D and 3D uranium oxo-silicates/germanates and some statistical aspects of uranyl coordination in oxo-salts. *Inorg. Chem.* 2019, *58*, 10333–10345.
17. Chen Y. H., Liu H. K., Chang W. J., Lii D., Lii K. H. High-temperature, high-pressure hydrothermal synthesis, characterization, and structural relationships of mixed-alkali metals uranyl silicates. *J. Solid State Chem.* 2016, *236*, 55–60.
18. Plaisier J. R., Ijdo D. J. W., de Mello D. C., Blasse G. Structure and luminescence of barium uranium disilicate ($BaUO_2Si_2O_6$). *Chem. Mater.* 1995, *7*, 738–743.
19. Betteridge P. W., Carruthers J. R., Cooper R. I., Watkin K. P., Watkin D. J. CRYSTALS version 12: software for guided crystal structure analysis. *J. Appl. Crystallogr.* 2003, *36*, 1487.
20. Farrugia L. J. WinGX suite for small-molecule single-crystal crystallography. *J. Appl. Crystallogr.* 1999, *32*, 837–838.
21. Dolomanov O. V., Bourhis L. J., Gildea R. J., Howard J. A. K., Puschmann H. OLEX2: A complete structure solution, refinement and analysis program. *J. Appl. Crystallogr.* 2009, *42*, 339–341.

22. Gagné O. C., Hawthorne F. C. Comprehensive derivation of bond-valence parameters for ion pairs involving oxygen. *Acta Crystallogr.* 2015, *B71*, 562–578.
23. Adams S. Relationship between bond valence and bond softness of alkali halides and chalcogenides. *Acta Crystallogr.* 2001, *B57*, 278–287.
24. Zachariasen W. H. Bond lengths in oxygen and halogen compounds of d and f elements. *J. Less-Common Met.* 1978, *62*, 1–7.
25. Wylie E. M., Burns P. C. Crystal structures of six new uranyl selenate and selenite compounds and their relationship with uranyl mineral structures. *Can. Mineral.* 2012, *50*, 147–157.
26. Juillerat C. A., Moore E. E., Besmann T., Zur Loye H. C. Observation of an unusual uranyl cation-cation interaction in the strongly fluorescent layered uranyl phosphates $Rb_6[(UO_2)_7O_4(PO_4)_4]$ and $Cs_6[(UO_2)_7O_4(PO_4)_4]$. *Inorg. Chem.* 2018, *57*, 3675–3678.
27. Plášil J. A novel sheet topology in the structure of kamitugaite, $PbAl[(UO_2)_5(PO_4)_{2.38}(AsO_4)_{0.62}O_2(OH)_2](H_2O)_{11.5}$. *J. Geosci-Czech* 2017, *62*, 253–260.
28. Deifel N. P., Holman K. T., Cahill C. L. PF6-hydrolysis as a route to unique uranium phosphate materials. *Chem. Comm.* 2008, 6037–6038; https://doi.org/10.1039/b813819b.
29. Walenta K., Hatert F., Theye Th., Lissner F., Roeller K. Nielsbohrite, a new potassium uranyl arsenate from the uranium deposit of Menzenschwand in the Southern Black Forest, Germany. *Eur. J. Mineral.* 2009, *21*, 515–520.
30. Burns P. C., Alexopoulos C. M., Hotchkiss P. J., Locock A. J. An unprecedented uranyl phosphate framework in the structure of $[(UO_2)_3(PO_4)O(OH)(H_2O)_2](H_2O)$. *Inorg. Chem.* 2004, *43*, 1816–1818.
31. Juillerat C. A., Kocevski V., Besmann T. M., zur Loye H.-C. Observation of the same new sheet topology in both the layered uranyl oxide-phosphate $Cs_{11}[(UO_2)_{12}(PO_4)_3O_{13}]$ and the layered uranyl oxyfluoride-phosphate $Rb_{11}[(UO_2)_{12}(PO_4)_3O_{12}F_2]$ prepared by flux crystal growth. *Front. Chem.* 2019, *7*, 1–10.

**Supplementary Material:** The online version of this article offers supplementary material (https://doi.org/10.1515/zkri-2023-0038).